

# 3D Spectroscopic Observations of Star-Forming Dwarf Galaxies

Peter M. Weilbacher, Luz Marina Cairós, Nicola Caon, Polychronis Papaderos

**Abstract** We give an introduction into the observational technique of *integral field* or *3D* spectroscopy. We discuss advantages and drawbacks of this type of observations and highlight a few science projects enabled by this method. In the second part we describe our 3D spectroscopic survey of Blue Compact Dwarf Galaxies. We show preliminary results from data taken with the VIMOS integral field unit and give an outlook on how automated spectral analysis and forthcoming instruments can provide a new view on star formation and associated processes in dwarf galaxies.

## 1 Integral Field Spectroscopy

Integral Field Spectroscopy (IFS) is a three-dimensional observing technique, producing a spectrum for every sampled element on the sky. The end result after data reduction is therefore typically a "datacube", with two spatial axes and the spectral direction. This method is therefore often called *3D Spectroscopy*.

---

Peter M. Weilbacher

Astrophysikalisches Institut Potsdam (AIP), An der Sternwarte 16, D-14482 Potsdam, Germany  
e-mail: pweilbacher@aip.de

Luz Marina Cairós

Astrophysikalisches Institut Potsdam (AIP), An der Sternwarte 16, D-14482 Potsdam, Germany

Nicola Caon

Instituto de Astrofísica de Canarias (IAC), C/ Vía Láctea, s/n E38205 - La Laguna (Tenerife), Spain

Polychronis Papaderos

Centro de Astrofísica da Universidade do Porto (CAUP), Rua das Estrelas 4150-762 Porto, Portugal

## 1.1 IFS basics

Unlike scanning techniques, an integral field unit (IFU) splits up the telescope focal plane into a series of elements (typically lenslets, fibers, or slicers, or a combination of them) and forms a pseudoslit from which the light is dispersed to be recorded on a CCD. Such an exposure includes all wavelengths and full spatial sampling and extent of the instrument, recorded at the same time and under the same (atmospheric) conditions. Hence, IFS is a very efficient observing scheme, especially if the objects of interest fit into the field of view of one pointing. This is also one of the drawbacks of IFS: the current instruments only cover a relatively small area on the sky, up to  $\sim 110''$  (as for VIRUS-P; [19]). The other disadvantage is that the information content of each exposure is extremely high, and depending on the instrument, it can take a long time to properly (re-)construct the datacube from the raw data. One can therefore say that in general, IFS shifts the effort from the time spent to carry out observing programs to the time required to do proper data reduction (and data analysis). But recently, more and more software packages are becoming available for IFS data reduction. Many instrument-specific pipelines are being maintained (at e.g. the ESO and Gemini observatories) but there are also more general reduction packages for fiber-based IFU data. The newest package which has been adapted to reduce data from almost ten of the most popular integral field instruments is P3D<sup>1</sup> [20].

Of course, IFS would not be rising in popularity, if there were not advantages that by far outweigh the difficulties, at least for selected scientific applications. Obviously, it enables bidimensional spectral coverage (as opposed to traditional slit spectroscopy) with all the advantages that implies: no slit effects or slit losses, no necessity to do (pre-)imaging of the same field, a spectral resolution that is independent of spatial coverage, possibility to correct for atmospheric dispersion and to bin the data spatially to gain S/N. IFS also has potentially long wavelength coverage (as compared to the Fabry-Perot technique) and, as said above, guarantees homogeneous conditions for the whole dataset (as opposed to scanning techniques).

## 1.2 IFS advantage: no slit effects

The problem of slit effects [see e.g. 2] (for a detailed discussion) is particularly troublesome for slit spectroscopy, which many astronomers are not aware of. If one observes one or more compact objects with a slit spectrograph under seeing conditions which cause a FWHM smaller than the slit width, velocities measured for each object depend on their centering within the slit. This can be corrected for stellar fields with precisely known star positions (as done by [17]). But for emission line kinematics of compact objects such a correction is not possible, unless a narrow-band image with sufficient spatial resolution exists, from which the exact positions

<sup>1</sup> Available from the project webpage <http://p3d.sourceforge.net>.

of all relevant emission line peaks can be determined. Emission line kinematics of e.g. star-forming dwarf galaxies derived using long-slits is therefore to be regarded with caution.

To give an example: if one observes  $H\alpha$  with a spectral resolution of  $R = 500$  at slit width of  $1''$ , the slit is effectively  $\sim 600 \text{ km s}^{-1}$  wide. At a resolution of  $R = 10000$  it still is  $\sim 30 \text{ km s}^{-1}$  wide. So, if one happens to observe a compact HII region in  $0''.5$  seeing with a  $1''$  slit and  $R = 10000$ , one on average makes an error of  $\pm 15 \text{ km s}^{-1}$  (for shifts of half the slit width the FWHM of the object is still within the slit) at each position along the slit. Rotation curves derived that way can look very much like disturbances caused by e.g. galaxy merging and lead to wrong interpretation of the galaxy at hand.

Most kinds of integral field spectrographs are insensitive to slit effects: instruments which use lenslets are insusceptible to this problem; fiber-based systems are less affected as fibers scramble the spatial signal sufficiently well. Only IFUs built using slicers with low spatial sampling can be affected. But then one can derive the spatial position of most objects within the field of view, allowing to correct for the instrumental shifts. Of course, instruments based on the Fabry-Perot principle are also immune. To derive emission line kinematics of any object one should therefore always choose to observe with an integral field spectrograph or a similar instrument that is not affected by slit effects.

### ***1.3 Analyses enabled by IFS***

Some kinds of analyses are only possible if one observes galaxies with IFS. Basically, one can create two-dimensional maps of many properties, which is not possible using slit spectroscopy. One can even create spatially resolved maps involving line ratios or equivalent widths (EWs) which is possible with Fabry-Perot instruments but expensive in terms of observing time. Typical IFS-based maps are those for extinction (Balmer decrement) and chemical abundances. Two-dimensional spectroscopy also allows to create color maps from which the effects of dust and contributions by emission line fluxes were removed; these can then be interpreted using photometric stellar population models without the need to build complex models involving extinction and line emission. Kinematical analyses are of course possible, but can be done using other observing methods. Another unique analysis enabled by IFU-observations is the search for spectral signatures across a galaxy. This is typically done for Wolf-Rayet features in star-forming objects.

Projects like SAURON (kinematics and stellar populations of nearby elliptical galaxies; [3, 13]) and SINS (properties of  $z \sim 2$  galaxies; [15, 14]) would not have been possible without integral field spectroscopy (and a well-managed team working on data reduction and analysis).

## 2 Studies of Blue Compact Dwarf galaxies with IFS

Among the many recent publications involving integral field spectroscopy of dwarf galaxies we want to highlight those of an ongoing, comprehensive study of Blue Compact Dwarf (BCD) galaxies. BCDs are dwarf starburst galaxies with low metallicity, often regarded as local counterparts of young galaxies observed at high-redshift. Although it became clear later on that the vast majority of these dwarf galaxies have an underlying old stellar population [9, 4], these objects are still the best nearby laboratories for exploring violent star formation and dwarf galaxy build up, including the feedback processes associated with it. Some among the many open questions which we try to address using IFS: What are the star-formation histories of BCDs? What is their dust content and distribution? Are there evolutionary connections between star-forming dwarfs and other types of dwarfs? What mechanisms trigger the starburst? Are interactions and mergers playing a role?

### 2.1 Project description

In our project (PI L. M. Cairós) we aim to thoroughly analyze a large sample of  $\gtrsim 40$  BCDs using integral field spectroscopy. Our targets are located in both hemispheres and cover a wide range in luminosity ( $-13.9 \lesssim M_B \lesssim -21.1$  mag). We observed BCDs over a wide metallicity ( $0.05 < Z_{\odot} < 0.85$ ) and morphology range [4]. Deep (optical) imaging in at least two bands is available for all our targets. By now we have acquired data from four instruments/telescopes: INTEGRAL (coupled to the WYFFOS spectrograph at WHT), PMAS (3.5m Calar Alto telescope), VIRUS-P (at the 2.7m McDonald telescope), and VIMOS (at the ESO VLT).

Our methodology involves a thorough analysis of the data of each object. We first build maps of emission line fluxes or equivalent widths for different line types (hydrogen Balmer lines, forbidden oxygen or sulfur lines, etc.). These maps allow us to localize the HII regions and investigate the luminosity, morphology, excitation mechanisms, extinction pattern, and kinematics of the ionized gas component. From maps of the continuum we can study the morphology of the underlying stellar component, undisturbed by line emission, and better assess its age structure. The Balmer decrement enables us to carry out a spatially resolved study of the intrinsic extinction. Further insights can be obtained from Wolf-Rayet features (based on the study of the emission lines in the spectral range  $4650 \dots 4690 \text{ \AA}$ ) which gives clues to the starburst age and the shape of the initial mass function. Metal emission lines can tell us about physical parameters of the gas and spatial variations of the chemical abundances. Using gas and stellar velocity fields we investigate the origin of starburst activity and estimate the total mass of the galaxy. Finally, we use spatially resolved spectral synthesis models to characterize the properties of stellar populations in the sample galaxies (see 3.1).

Some of our data taken with INTEGRAL and PMAS has already been published. An initial investigation of five galaxies with INTEGRAL was presented in [16],

and a paper first showing the potential of the PMAS data for the case of Mrk 1418 appeared as [7]. The PMAS data on Mrk 409 was thoroughly exploited by [5] and a general presentation of the objects observed so far with PMAS was published as [6]. A further description of the sub-sample of BCDs observed with the PMAS and VIRUS-P instruments can also be found in [8, this volume]. All these papers show results that would have been impossible to acquire with other observing techniques.

## 2.2 VIMOS data

Nine southern galaxies of our sample were so far observed with the VIMOS spectrograph on the 8.2m ESO VLT. This dataset contains our deepest exposures with the highest spectral resolution ( $R \sim 2600$ ). We used the HRblue and HRorange grisms to cover most of the optical wavelength range from 4300 to 7400 Å. We used the setup with low spatial resolution ( $0.67'' \text{ px}^{-1}$ ) that was well matched to the seeing and allowed to cover  $\sim 27'' \times 27''$  per target. Our observing strategy involved several dithered exposures per galaxy and grism, to fill in bad spatial elements (spaxels) and to aid sky subtraction. This increased the complexity of the data reduction, since the combination of multiple dithered exposures into a full datacube is not supported by any existing processing tool.

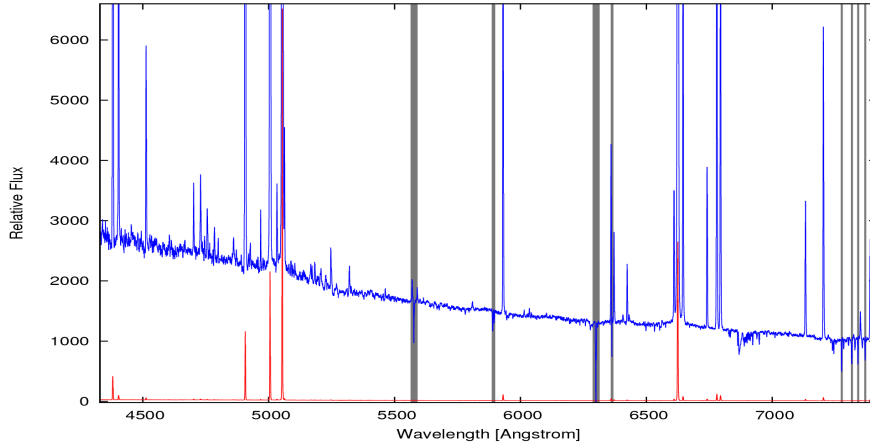


**Fig. 1** Spectrum of Tol 1924-416: this spectrum was integrated over the 80 central spectral elements of our VIMOS data. It shows many faint He and metal lines with detections at good S/N. The lower spectrum is the same as the upper one but scaled down  $100\times$  to show the bright emission lines. Grey vertical semitransparent areas indicate sky emission lines that could not be subtracted perfectly.

Here, we show preliminary results of one object of our VIMOS sample, Tol 1924-416. Figure 1 shows an integrated spectrum of the central part of Tol 1924-416. This

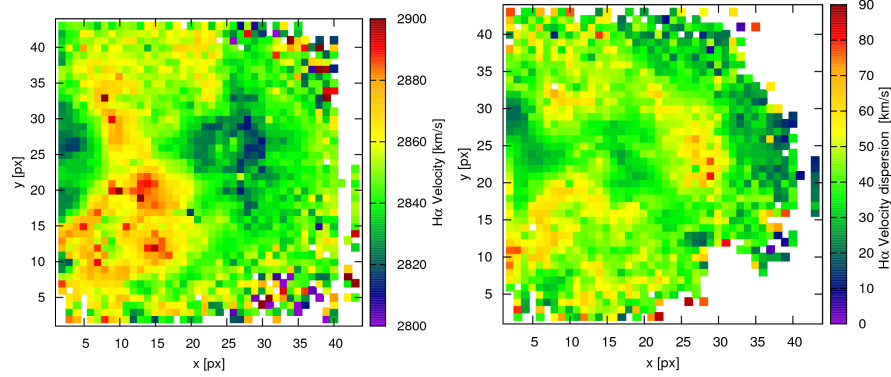


**Fig. 2** Kinematical maps of Tol 1924-416: *left* is the velocity field as derived from  $H\alpha$ , *right* is the velocity dispersion measured from the same line.

high S/N spectrum shows many faint Helium and metal lines that are not commonly seen in BCDs. Figure 2 presents maps of velocity and velocity dispersion as derived from the  $H\alpha$  emission line. While the emission line morphology is similar to the broad-band appearance, the velocity structure is very complex. While local starburst-driven winds might contribute to this structure, it is tempting to take it as a sign of merging, similar to what previous investigations of this galaxy concluded from optical broad- and narrow-band observations [18, 12]. Derivation of stellar velocities in this galaxy, to confirm or disprove this view, are difficult as only very few spaxels show absorption.

### 3 Conclusions & Outlook

In this article we described the technique of integral field spectroscopy that provides an unbiased and unrestricted view on dwarf galaxies: from the same data, taken under nearly identical conditions, one can derive kinematics (gaseous and possibly stellar) and physical properties of the warm interstellar medium (e.g. metallicity, density), and study the stellar populations in two dimensions. We briefly outlined a project investigating the structure and evolution of BCDs with IFS and showed preliminary results for one galaxy from our sample.

But most of the findings enabled by 3D spectroscopy are probably still to come. Next, we briefly discuss two topics that will help to further exploit existing data and to produce major new results, in the research area of dwarf galaxies and beyond.

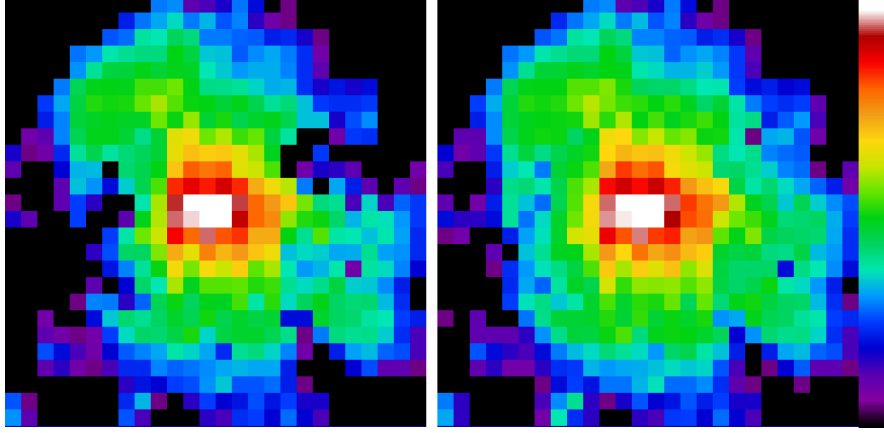


**Fig. 3** Automated stellar continuum analysis of VIRUS-P data for the BCD III Zw 102: the *left* and *right* panels show, respectively, the  $H\beta$  map of the galaxy prior to and after correction for underlying stellar absorption.

### 3.1 Automated spectral analysis

Most IFS-based investigations so far analyze the integrated spectrum of multiple regions of interest, or perform Gaussian emission line fitting to individual spaxels, leaving unexploited the information provided by stellar absorption lines. As deeper data gets available, the latter will become more accessible and can be used, especially for kinematical studies.

Another approach is to use spectral synthesis and analysis tools to model the stellar continuum spaxel by spaxel. This yields a twofold benefit, as it allows for insights into the stellar populations and for the correction for underlying stellar absorption, thereby an improvement on the accuracy of emission line measurements. Especially Balmer line fluxes usually have to be corrected for underlying stellar absorption. The subtraction of the best-fitting stellar model offers an effective means for accomplishing this task.

As an example, we show in Fig. 3 preliminary results from the analysis of our VIRUS-P data for the BCD III Zw 102 (Cairós et al., in prep.). We used the STARLIGHT code [10, 11] to generate a stellar continuum fit at each position. Figure 3 shows the  $H\beta$  flux before and after correction for underlying stellar absorption using the best-fitting stellar model for each spaxel. It can be seen that the artificial depression in the  $H\beta$  flux distribution in southeastern and northwestern direction could be efficiently rectified this way (Papaderos et al., in prep.).

### 3.2 New instruments

Several major new IFSs are scheduled to come on-line in the next years. At the ESO VLT, all new instruments will be based on the integral field principle or will at least contain an ancillary IFU-mode. The major IFSs to become available at ESO are KMOS, a near-infrared spectrograph with 24 small IFUs, and MUSE, an optical instrument. The VIRUS instrument in development for the HET at McDonald observatory will provide simultaneous (but not contiguous) spectral coverage of an area of  $30'' \times 1''$  using a setup of up to  $\sim 150$  fiber bundles.

Of these, the **Multi Unit Spectroscopic Explorer** (MUSE; [1]) will probably be the most powerful instrument to further drive ahead the field of nearby star-forming dwarf galaxies. It is currently being built as one of the 2nd generation instruments for the ESO VLT and will see first light in 2012. Its  $1' \times 1'$  field of view at  $0''.2$  sampling, long wavelength range of (4650) 4800...9300 Å, relatively high spectral resolution ( $R \sim 3000$ ), and high throughput should make it an ideal multi-purpose instrument. After first light, it will be enhanced with an adaptive optics module to in the end allow near-diffraction limited spectroscopy in a  $7''.5 \times 7''.5$  field with a  $0''.025$  sampling.

**Acknowledgements** PMW acknowledges support by the German Verbundforschung through the MUSE/D3Dnet project (grant 05A08BA1). PP is supported by a Ciencia 2008 contract, funded by FCT/MCTES (Portugal) and POPH/FSE (EC).

### References

- [1] Bacon, R. et al.: The MUSE second-generation VLT instrument *SPIE* **7735** (2010).
- [2] Bacon, R. et al.: 3D spectrography at high spatial resolution. I. Concept and realization of the integral field spectrograph TIGER. *A&AS* **113**, 347 (1995)
- [3] Bacon, R. et al.: The SAURON project - I. The panoramic integral-field spectrograph. *MNRAS* **326**, 23 (2001).
- [4] Cairós, L., Vílchez, J., González Pérez, J., Iglesias-Páramo, J., Caon, N.: Multiband Analysis of a Sample of Blue Compact Dwarf Galaxies. I. Surface Brightness Distribution, Morphology, and Structural Parameters. *ApJS* **133**, 321 (2001)
- [5] Cairós, L.M. et al.: New Light in Star-Forming Dwarf Galaxies: The PMAS Integral Field View of the Blue Compact Dwarf Galaxy Mrk 409. *ApJ* **707**, 1676 (2009).
- [6] Cairós, L.M. et al.: Mapping the properties of blue compact dwarf galaxies: integral field spectroscopy with PMAS. *A&A* **520**, A90 (2010).
- [7] Cairós, L.M. et al.: Mapping the starburst in blue compact dwarf galaxies. PMAS integral field spectroscopy of Mrk 1418. *A&A* **507**, 1291 (2009).



- [8] Cairós, L.M. et al.: Mapping the properties of Blue Compact Dwarf galaxies by means of Integral Field Spectroscopy. this volume.
- [9] Papaderos, P., Loose, H.-H., Fricke, K.J., Thuan, T.X.: Optical structure and star formation in blue compact dwarf galaxies. II. Relations between photometric components and evolutionary implications. *A&A* **314**, 59 (1996)
- [10] Cid Fernandes, R. et al.: The star formation history of Seyfert 2 nuclei. *MNRAS* **355**, 273 (2004).
- [11] Cid Fernandes, R. et al.: Semi-empirical analysis of Sloan Digital Sky Survey galaxies - I. Spectral synthesis method. *MNRAS* **358**, 363 (2005).
- [12] Doublier, V., Caulet, A., Comte, G.: Multi-spectral study of a new sample of Blue Compact Dwarf Galaxies. II. B and R surface photometry of 22 southern objects. *A&AS* **138**, 213 (1999).
- [13] Emsellem, E. et al.: The SAURON project - IX. A kinematic classification for early-type galaxies. *MNRAS* **379**, 401 (2007).
- [14] Förster Schreiber, N.M. et al.: The SINS Survey: SINFONI Integral Field Spectroscopy of  $z \sim 2$  Star-forming Galaxies. *ApJ* **706**, 1364 (2009).
- [15] Förster Schreiber, N.M. et al.: SINFONI Integral Field Spectroscopy of  $z \sim 2$  UV-selected Galaxies: Rotation Curves and Dynamical Evolution. *ApJ* **645**, 1062 (2006).
- [16] García-Lorenzo, B. et al.: Integral Field Spectroscopy of Blue Compact Dwarf Galaxies. *ApJ* **677**, 201 (2008).
- [17] Gerssen, J. et al.: Hubble Space Telescope Evidence for an Intermediate-Mass Black Hole in the Globular Cluster M15. II. Kinematic Analysis and Dynamical Modeling. *AJ* **124**, 3270 (2002).
- [18] Heisler, C.A., Vader, J.P.: Galaxies with Spectral Energy Distributions Peaking Near 60 micron. III. H(alpha) Imaging. *AJ* **110**, 87 (1995).
- [19] Hill, G.J. et al.: Design, construction, and performance of VIRUS-P: the prototype of a highly replicated integral-field spectrograph for HET. *SPIE* **7014** (2008).
- [20] Sandin, C., Becker, T., Roth, M.M., Gerssen, J., Monreal-Ibero, A., Böhm, P., Weilbacher, P.: P3D: a general data-reduction tool for fiber-fed integral-field spectrographs. *A&A* **515**, A35 (2010). URL <http://p3d.sourceforge.net>